AB INITIO SCF MO STUDY OF $H_6SI_2O_7$ AT SIMULATED HIGH PRESSURE

by

© NANCY LEE ROSS

B.Sci., Virginia Polytechnic Institute and State University

A THESIS SUBMITTED IN PARTIAL FULFILLMENT OF

THE REQUIREMENTS FOR THE DEGREE OF

MASTER OF SCIENCE

in

THE FACULTY OF GRADUATE STUDIES

Department of Geological Sciences

We accept this thesis as conforming

to the required standard

THE UNIVERSITY OF BRITISH COLUMBIA

August 1981

In presenting this thesis in partial fulfilment of the requirements for an advanced degree at the University of British Columbia, I agree that the Library shall make it freely available for reference and study. I further agree that permission for extensive copying of this thesis for scholarly purposes may be granted by the head of my department or by his or her representatives. It is understood that copying or publication of this thesis for financial gain shall not be allowed without my written permission.

Department of Geological Sciences

The University of British Columbia
2075 Wesbrook Place
Vancouver, Canada
V6T 1W5

Date August 6, 1981

ABSTRACT

Molecular orbital calculations have been successively applied to mineralogical studies of equilibrium molecular geometry, electronic charge distributions, electronic spectra and bulk modulus calculations. To date, these studies have modelled bonding at atmospheric pressure. With the ever increasing interest in high pressure phases and mantle mineralogy, bonding studies of molecular groups at simulated high pressure can be an invaluable aid to understanding high pressure crystal chemistry, bond energetics and electronic spectra.

This investigation tests the feasibility of various models to simulate pressure in *ab initio* SCF MO calculations on common metal-oxygen polyhedra. Pressure is simulated in the cluster, $H_6Si_2O_7$, by systematically stepping helium atoms directed along the Si-O bridging vectors toward the bridging oxygen. Changes in the Si-O bond lengths, SiOSi angles and Si-O force constants are monitored with increasing pressure.

For an increase of 60 kbar pressure, the Si-O bond length and SiOSi angle decrease 0.30% and 4.5%, respectively, which compares well with the 0.30% and 6.6% decrease observed in α-quartz for a similar increment of pressure. The linear correlation of Si-O bond length and -sec(SiOSi), known to occur at one bar, holds at elevated pressure. In addition, the Si-O stretching and SiOSi bending force constants show a percentage increase in the ratio 1:6 up to an estimated

pressure of 140 kbar.

TABLE OF CONTENTS

LIST OF TABLES

LIST OF FIGURES

ACKNOWLEDGEMENTS

Sincere thanks are extended to Dr. E.P. Meagher for his guidance, support and encouragement throughout this study. This work was supported by the National Science and Engineering Research Council with NSERC grant 67-7061 and summer grants were provided by the NAHS. The cooperation of the computing centre at the University of British Columbia is also gratefully acknowledged.

Appreciation is expressed to Dr. G.V. Gibbs for introducing me to the exciting world of molecular orbital theory and to Monique Roussy for her many fruitful discussions.

Finally I thank Gord Hodge for his deft hand at draughting and his concern for the aesthetic appeal of all illustrations used in the text.

I. INTRODUCTION

Significant advances have been made in the past twenty five years with regards to the accurate determination of silicate structures which have, in turn, supplied a wealth of data for crystal chemical investigations of this geologically important mineral group. For the most part, these investigations have dealt with structural variations as a function of substituent cation radius, temperature, and in recent years, pressure (Papike *et al.*, 1969; Cameron *et al.*, 1973; Levien and Prewitt, 1981).

Until recently, investigations dealing with the chemical bonding in silicate minerals have been few in number and have been based mainly on the electrostatic model (Whittaker, 1971; Ohashi and Burnham, 1972). With the general knowledge that silicates have a high covalent character in their chemical bonding (Pauling, 1981), there has been a trend in the past decade toward utilizing molecular orbital methods in silicate bonding studies. In particular, there has been a concerted effort to understand the stereochemistry of silicates using molecular orbital formalisms ranging from the semi-empirical extended Huckel method (Louisnathan and Gibbs, 1972) and the CNDO/2 method (Meagher *et al.*, 1979) to the more sophisticated self-consistent field (SCF) *ab initio* method (Newton and Gibbs, 1980).

In addition to the success of the molecular orbital method in stereochemical studies, it has also been applied successively to bulk modulus calculations (Newton et al., 1980) and to the interpretation of absorption, emission and photoelectronic spectra in silica and silicate minerals (Tossell, 1973, 1979; Dejong and Brown, 1980). The agreement between molecular orbital calculations and observed values for silicates supports the view that isolated molecular groups possess local bonding forces that are similar to those found in three dimensional solids.

To date, these studies have modelled bonding at atmospheric pressure and molecular orbital calculations have not, as a rule, been applied to thermodynamic properties of minerals. The quantities K (bulk modulus) and dK/dP (first derivative of the bulk modulus with respect to pressure) are important parameters in the equations of state employed in geophysical research and in high pressure crystal chemical studies of minerals. Unfortunately these quantities are difficult to determine experimentally, especially at high confining pressures. Recent advances in crystal structure determinations at high pressures by x-ray diffraction methods have yielded some valuable data. The experiments are currently limited, however, to approximately 60 kbars pressure and foreseeable advances will extend the pressure range to 200 kbars at best.

Over the past fifty years, various empirical relationships between K and molar volumes of solids have been proposed. Recently investigators have proposed an empirical relationship between the bulk modulus of cation-anion polyhedra (Kp) and the mean cation-anion distances at one atmosphere pressure (Hazen and Finger, 1979). They suggest that in order to predict K of a complex solid one must know the Kp values of the component polyhedra in the solid. Although these relationships lend themselves to predicting compressibilities of simple solids at low confining pressures, they are not successful for more complex solids or for predictions of K at high confining pressures.

An alternative approach is proposed whereby the quantities Kp and d(Kp)/dP will be computed utilizing the relationship,

$$
\begin{aligned}
Kp &= V(\partial^2E/\partial r^2)(dr/dV)^2 \\
&= V(k_s(dr/dV)^2 \qquad (1)
\end{aligned}
$$

where V is the volume of the polyhedron, r is the cation-anion distance, E is the total energy and k_s is the stretching force constant.

This study is the first in a series investigating compressibilities of the more common metal-oxide polyhedra found in the earth's crust and mantle. The groundwork for future studies is laid by testing models for simulation of pressure with SCF molecular orbital calculations. Among the molecular clusters of geological interest is the Si_2O_7 dimer. In this study, we monitor changes in the stereochemistry of $H_6Si_2O_7$ as a function of pressure as well as changes in the stretching and bending force constants of the SiOSi linkage with pressure. The computation of polyhedral bulk moduli and their variation with pressure will be completed in work now underway on the SiO_4 and AlO_4 tetrahedra and in future work on octahedral oxyanion clusters of magnesium, aluminum and silicon. Investigations such as the above provide insights into the atomic responses to pressure in silicate structures.

II. MOLECULAR ORBITAL METHOD

Description

The molecular orbital (MO) method forms the underlying basis for the calculations in this study. The MO method provides an approximate solution to the Schrödinger wave equation,

$$H\Psi=E\Psi \tag{2}$$

for a many-electron molecule or cluster of atoms. This is equivalent to an eigenvector (Ψ) eigenvalue (E) problem. The central premise in MO theory is that the complex many-electron wavefunction, Ψ, can be approximated as an antisymmetrized product of one-electron wavefunctions, ψ_m, called moleculer orbitals,

$$\Psi_{many\text{-}electron}=\prod_{m=1}^{n} \psi_m, \tag{3}$$

where n is the total number of electrons in the system. The optimal wavefunction, Ψ (also known as the Hartree-Fock wavefunction), will be the one which minimizes the total energy for an atomic cluster in its ground state, E_{mol},

$$E_{mol} = \int \Psi^{*} H \Psi d\tau \tag{4}$$

where Ψ is the many-electron wavefunction defined in (3) and H is the many-electron Hamiltonian operator.

Incorporated in the hamiltonian are the kinetic and potential energies of the nuclei and electrons in the atomic group. If the Born-Oppenheimer approximation is accepted, whereby the nuclei are considered fixed, the hamiltonian for an atomic cluster with m nuclei and i,j electrons can be expressed in the following way,

$$H = \sum_{i} (-\hbar^2/2M)\nabla_i^2 - \sum_{i}\sum_{m} (Z_m e^2/r_{im}) + \sum_{i<j}\sum (e^2/r_{ij}) \quad , \tag{5}$$

where ∇_i is the Laplacian operator. The first term represents the kinetic energy of the electrons, the second term represents their potential energies due to attraction with the nuclei and the third term represents the repulsion between electrons.

The hamiltonian is frequently divided into one-electron terms, H , and two-electron terms, e^2/r_{ij}, such that

$$H = \sum_{i} H_i + \sum_{i<j}\sum (e^2/r_{ij}) . \tag{6}$$

The energy relating to the one-electron operator (also known as the core hamiltonian) is

$$E_m = \int \psi_m^*(i) H_i \psi_m(i) d\tau_i , \tag{7}$$

where E represents the sum of the kinetic and potential energy due to an electron occupying orbital ψ_m. A typical two-electron term representing the repulsive potential energy between electrons i,j is

$$\begin{aligned} V &= \iint \psi_m^*(i)\psi_m(i)\ (e^2/r_{ij})\ \psi_n^*(j)\psi_n(j)\ d\tau_i d\tau_j\ - \\ &\quad \iint \psi_m^*(i)\psi_n(i)\ (e^2/r_{ij})\ \psi_m^*(j)\psi_n(j)\ d\tau_i d\tau_j \\ &= J_{mn} - K_{mn}, \end{aligned} \tag{8}$$

where J_{mn} is the Coulomb repulsive energy and K_{mn} is the exchange energy. The total energy of the system can be expressed as

$$E_T = \sum_m E_m + \sum_{m<n}\sum J_{mn} - \sum_{m<n}\sum K_{mn} \tag{9}$$

for molecular orbitals m and n.

After defining the hamiltonian, suitable wavefunctions , ψ_m, must be found which satisfy the one-electron Schrödinger equation,

$$F\psi_m = \epsilon_m \psi_m, \tag{10}$$

where the operator F is the Hartree-Fock or effective one-electron Hamiltonian and ϵ_m is the one-electron energy. In other words, there will be a series of ψ_m which are eigenvectors of the linear operator F, each with a unique energy ϵ_m. In practice the molecular orbitals, ψ_m, are expanded in terms of a convenient basis set of N atomic orbitals, ϕ_r, centered on the various atoms of the molecule,

$$\psi_m = \sum_{r=1}^{N} \phi_r c_{rm}. \tag{11}$$

That is, the molecular orbitals are expressed as a linear combination of atomic orbitals (LCAO). The atomic orbitals can be any general set of specified single-electron functions.

The best approximations for the wavefunctions, ψ_m, will be those that give the lowest energies, ϵ_m. This is in accordance with the Variation Principle which states that the value of the calculated energy is always greater than or equal to the true ground state electronic energy. The problem is reduced to finding the set of coefficients, c_{rm}, that yields the lowest energy. This is done by minimizing the energy with respect to each of the coefficients. Following this method, the coefficients must satisfy equations which can be written in matrix form,

$$\underset{\sim}{F}\underset{\sim}{C}_m = \epsilon_m \underset{\sim}{S}\underset{\sim}{C}_m \tag{12}$$

where $\underset{\sim}{C}_m$ is a column vector of MO coefficients, $\underset{\sim}{F}$ is the matrix whose elements are defined as

$$F_{rt} = \int \phi_r F \phi_t d\tau \tag{13}$$

where F=H+J-K and $\underset{\sim}{S}$ is the overlap matrix with elements,

$$S_{rt} = \int \phi_r \phi_t d\tau . \tag{14}$$

The secular equations (or Roothaan equations),

$$FC=SCE \tag{15}$$

are solved iteratively with successively better c_{rm} and E values until convergence (self-consistency) is achieved.

In addition to the total molecular energy, we are interested in the orbital population analysis which partitions the total number of electrons in the system into various atomic and bond contributions (Mulliken, 1955). Integration of the total molecular orbital density function

$$\rho(\underset{\sim}{r}) = \sum_{m=1}^{n} \psi_m^*(\underset{\sim}{r}) \psi_m(\underset{\sim}{r}), \tag{16}$$

expanded in terms of the atomic orbital basis,

$$\rho(\underset{\sim}{r}) = \sum_{st}^{N} \sum_{r=1}^{n} c_{sr} c_{tr} \phi_s^*(\underset{\sim}{r}) \phi_t(\underset{\sim}{r}), \tag{17}$$

yields the total number of elecrons, n:

$$n = \sum_{st}^{N} \sum_{r=1}^{n} c_{sr} c_{tr} S_{st} . \qquad (18)$$

The Mulliken bond overlap population for a pair of atoms, s-t, is defined by

$$n(s-t) = \sum_{r=1}^{n} c_{sr} c_{tr} S_{st} \qquad (19)$$

when summed over all atomic orbitals on center s and all atomic orbitals on center t. If the overlap population between two atoms is positive, they are bonded; if negative, they are antibonded.

The atomic orbital population for an atom s, q(s), is obtained by summing the quantity n(s-t) over all atomic orbitals on t:

$$q(s) = \sum_{t}^{T} n(s-t). \qquad (20)$$

The atomic charge of atom s, Q(s), is defined by

$$Q(s) = q_0(s) - q(s) \qquad (21)$$

where $q_0(s)$ is the total number of electrons in the ground state of the free, neutral atom s.

MO Methods

Molecular orbital calculations can be classified into two general categories: "approximate molecular orbital methods" and " *ab initio* " calculations.In the approximate MO methods, a large portion of the electron integrals involved in the calculation are approximated by known atomic quantities and by the use of "semi-empirical" expressions for elements in the Hartree-Fock matrix. The approximations adopted for these integrals and the semi-empirical expressions are evaluated with respect to their ability to predict experimental results.

One of the better-known approximate MO methods is the Complete Neglect of Differential Overlap (CNDO/2) method (Pople *et al*. , 1965). As its name implies, all electron repulsion integrals of the "differential overlap" type[1] are neglected. In addition, semi-empirical expressions are used to calculate the elements of the Hartree-Fock matrix. CNDO/2 molecular orbital calculations on disiloxane (Tossell and Gibbs, 1977) and pyrosilicic acid (Meagher *et al*. ,1979) yield minimum energy SiOSi angles in close agreement with observed values for silica polymorphs and glass. However, CNDO/2 calculations tend to drastically overestimate bond lengths for second row elements (Marsh and Gordon, 1976).

---

[1]An example of an elecron repulsion integral of the differential overlap type is $\iint \phi_r(1)\phi_s(1)(1/r_{12})\phi_t(2)\phi_u(2)d\mathbf{r}_1 d\mathbf{r}_2$ where ϕ_r, ϕ_s, ϕ_t, and ϕ_u are atomic orbitals.

In recent years, we have seen the development of <u>ab initio</u> SCF MO calculations and computer programs using Gaussian expansions of Slater-type orbitals. Unlike the approximate MO methods, <u>ab</u> <u>initio</u> calculations attempt to solve the full electronic Schrödinger equaton for a many-electron system. After defining the atomic positions and wave functions, all atomic overlap integrals, S_{rs}, are calculated. The kinetic and potential one-electron integrals which make up the core hamiltonian are evaluated next. Calculation of the two-electron integrals follows. The use of Gaussian-type wavefunctions for the atomic orbitals expedites the computation of these integrals. An initial guess of the Hartree-Fock matrix is made through a Hückel or extended Hückel approximation[2] or through diagonalization of the core hamiltonian. With the approximated Hartree-Fock matrix, the eigenvalues (or molecular orbital energies, ϵ_m) and eigenvectors (c_{rm}'s) are solved. With successively better coefficients and energy values, the secular equations (15) are solved iteratively until convergence is achieved.

<u>Ab</u> <u>initio</u> computations enable us to solve for equilibrium bond lengths and angles for molecules involving first and second row elements with a high degree of accuracy (Collins <u>et al.</u>, 1976). Optimized T-O distances and TOT angles, for

---

[2]With the extended Huckel approximation, the elements of the Hartree-Fock matrix are approximated with the Valence Orbital Ionization Potential (VOIP):
F =VOIP(u) ; F =K(VOIP(u)+VOIP(v))

example, compare well with local geometries in silica polymorphs, silicates, and siloxanes (Meagher _et al._, 1979;Newton and Gibbs, 1980). Furthermore, _ab initio_ calculations of quadratic force constants on a large number of polyatomic molecules satisfactorily account for nearly all experimental trends (Newton _et al._, 1970). For these reasons, _ab initio_ calculations were used in this study.

III. CALCULATIONS

Ab initio SCF molecular orbital calculations were undertaken with the Gaussian 76 computer program (Binkley *et al.*, 1978). Throughout this study, a minimal basis set, ϕ_r, was adopted in which each atomic orbital of the constituent atoms is represented by a single Slater-type orbital (STO) basis function. For example, we are dealing with nine STO basis functions for silicon and five STO basis functions for oxygen. To ease the computation of the two-electron integrals, the STO functions are, in turn, expanded as Gaussian-type orbitals (GTO's) (Hehre *et al.*, 1969). In the minimal basis set calculations used in this study (referred to as a minimal STO-3G basis set), each STO is represented by a linear combination of three Gaussian functions. Newton and Gibbs (1980) and Gibbs *et al.* (1981) have shown that a STO-3G minimal basis set is sufficient when studying the bond length and angle relationships for $H_6Si_2O_7$.

Molecular orbital calculations lend themselves readily to the evaluation of force constants (Newton *et al.*, 1979). The potential energy is expanded in terms of q,

$$E = E_0 + (\partial E/\partial q)q + 0.5(\partial^2 E/\partial q^2)q^2 + \cdots \qquad (22)$$

which is either the displacement from the equilibrium bond length, $r-r_0$, or angle, $\theta-\theta_0$, depending on whether a stretching force constant , k_s, or bending force constant, k_δ, is being calculated. In this study, r refers to the bridging Si-O bond length and θ is the SiOSi angle; r_0 and θ_0 are their respective equilibrium values. By definition, the quadratic force constant is twice the coefficient of the quadratic term:

$$k_s = (\partial^2 E/\partial q^2)\ \mathrm{Nm}^{-1} \tag{23}$$

$$k_\delta = (\partial^2 E/\partial q^2)/r^2\ \mathrm{Nm}^{-1} \tag{24}$$

where q qnd r are defined above. Thus the force constants are found directly by fitting a parabola to the potential energy curve. Increments of 0.01 Å about the equilibrium bond length and 2^0 about the equilibrium bridging angle were used to fit the parabola. With ranges of 0.05 Å and 8^0 about the equilibrium bond length and bridging angle, higher order terms in the expansion of the potential energy (22) were found to be insignificant. The definition of the bending force constant given above (24) is preferred because it yields the same dimensions (force/length) as the stretching force constant.

Three principal vibrational frequencies for the pyrosilicic acid molecule can be determined from the Si-O stretching and SiOSi bending force constants by following the method outlined by Herzberg (1945) for a XY_2 molecule. Treating the cluster as an XY_2 molecule, $(O(H_3SiO_3)_2)$, and assuming a valence force field model , we can express the potential energy as

$$E' = 0.5k_s qr^2 + 0.5k_\delta q\theta^2 \tag{25}$$

where qr is the displacement from the equilibrium bond length and $q\theta$ is the displacement from the equilibrium bridging angle. The valence force model assumes that there are no cross terms in the potential energy if it is expressed in terms of qr and $q\theta$. With the potential energy defined by (24), we can derive the following equations (Herzberg, 1945; p.169):

$$4\pi^2\nu_a^2 = (1 + (2m_Y/m_X)\ \sin^2(\theta_0/2)\ )\ k_s/m_Y \tag{26}$$

$$4\pi^2(\nu_s^2+\nu_b^2) = (1 + (2m_Y/m_X)\ \cos^2(\theta_0/2)\ )\ k_s/m_Y + (1 + (2m_Y/m_X)\ \sin^2(\theta_0/2)\ )\ 2k_\delta/m_Y \tag{27}$$

$$16\pi^4\nu_s^2\nu_b^2 = 2(1 + (2m_Y/m_X)\ )\ k_s k_\delta/m_Y^2 \tag{28}$$

where ν_s, ν_a and ν_b are the symmetric Si-O stretching, antisymmetric Si-O stretching and SiOSi bending frequencies, respectively; m_X is the mass of X (O), m_Y is the mass of Y (H_3OSi_3) and all other terms have been defined previously. Equations (26),(27) and (28) are solved simultaneously for ν_s, ν_a and ν_b.

IV. MODELS

Basically two different models were used in an effort to simulate elevated pressures in our calculations. In the initial model, which we will refer to as model I, pressure was simulated by simply locking the Si...Si distance at successively shorter values while maintaining a straight SiOSi angle. This model has restricted applications because of the need to maintain a straight SiOSi angle. However, model I was useful in comparing symmetric and asymmetric stretching force constants at one bar and asymmetric force constants at elevated pressures for the clusters $H_6Si_2O_7$, $H_6Al_2O_7^{-2}$, $H_{12}Si_5O_4$ and $H_{12}AlSi_4O_4^{-1}$. The symmetric force constants were calculated by keeping the bridging oxygen immobile while monitoring the changes in energy as the Si atoms were brought in toward the oxygen. The asymmetric force constants, on the other hand, were calculated by maintaining a constant Si...Si distance while monitoring the changes in energy as the bridging oxygen was oscillated. We also used model I to study the effect of polymerization on the Si-O force constant as well as the effect that substituting aluminum for silicon has upon the stretching force constants at one bar and as a function of pressure.

In all of the clusters studied with model I, staggered conformations were used and the SiOSi and AlOSi angles were maintained at 180°. In the $H_6Si_2O_7$ cluster, the O-H bond lengths were 0.96 Å while the SiOH and OSiO angles were locked at 109.47° , respectively (Figure 1). In the larger clusters, the OSiH and OAlH angles were 109.47° while the Si-H distances were locked at 1.49 Å. Tetrahedral, T_d , symmetry was maintained within the SiO_4 and AlO_4 tetrahedra throughout all computations.

In the second model, which we will refer to as model II, pressure was simulated about an $H_6Si_2O_7$ cluster by placing inert helium atoms along the Si-O bridging vector and systematically stepping the two heliums toward the bridging oxygen. This model allows for pressure simulation at bent SiOSi angles and is more precisely a uniaxial stress directed along the Si-O vectors.

The $H_6Si_2O_7$ dimer (Figure 2) was placed in a staggered conformation with O-H distances, d(O-H), and Si-O nonbridging bond lengths, d($Si-O_b$), of 0.96 Å and 1.65 Å, respectively. The OSiO and SiOH angles were likewise maintained at 109.47° and 180° , respectively, throughout all computations.

At one atmosphere, the equilibrium distances were the same with or without the helium atoms. At elevated pressures, we found that the Mulliken bond overlap populations between helium and nonbridging oxygens, n($He-O_{nb}$), and helium and silicon, n(He-Si), were never greater than 0.004 and 0.007, respectively.

Whereas model I yields asymmetric stretching force constants at elevated pressure, model II yields symmetric stretching force constants at one bar and at pressure. The

Figure 1. Molecular conformation for the dimers studied with model I (note the straight bridging angle); pressure is simulated by decreasing the intertetrahedral distance.

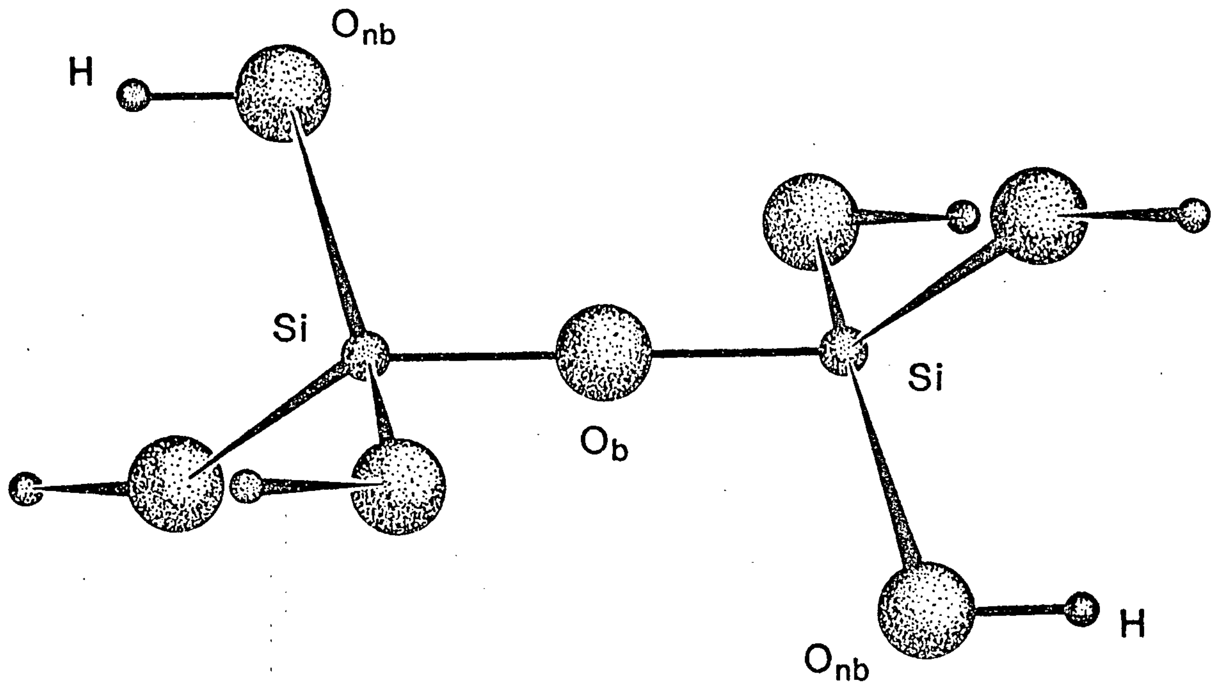

Figure 2. Molecular conformation for $H_6Si_2O_7$ when studied with model II. Note the bent bridging angle and positioning of helium atoms used to simulate pressure by systematically decreasing the $d(He-O_b)$ distances.

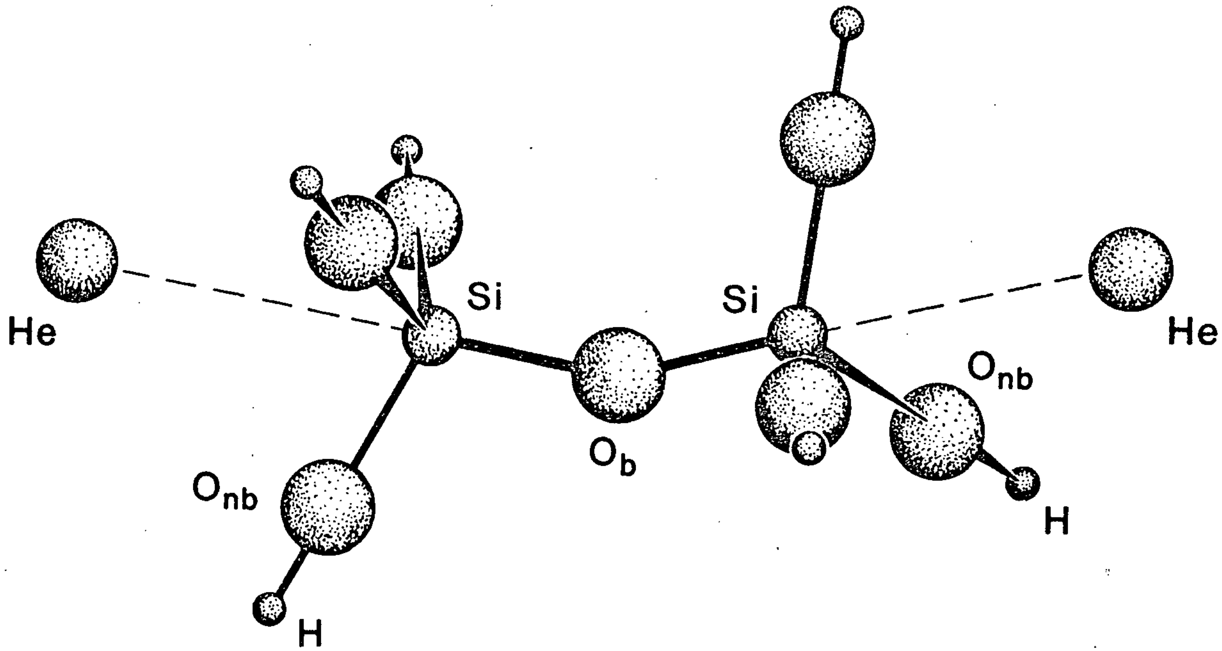

following were studied with model II: 1) changes in the equilibrium stereochemistry of $H_6Si_2O_7$ as a function of pressure; 2) changes in the stretching and bending force constants with pressure; and 3) the total potential energy as a function of bridging bond lengths and angles at elevated pressures. Model II is preferred because the bridging angle energetics as well as the bridging bond energetics can be studied as pressure is increased.

V. RESULTS AND DISCUSSION

Model I

As stated, model I provides a means of comparing the symmetric, k_s, and asymmetric, k_a, stretching force constants. At one bar, the calculated k_s and k_a for $H_6Si_2O_7$ [3] are 774 Nm^{-1} and 861 Nm^{-1}, respectively. Similarly, the asymmetric stretching force constant for $H_6Al_2O_7^{-2}$ [4], 630 Nm^{-1}, is lower than the symmetric stretching force constant, 715 Nm^{-1}. These results conflict with calculations based on infrared and raman spectroscopic data for a Si_2O_7 group with a linear bridge (Lazarev, 1972). The calculated asymmetric, ν_a, and symmetric, ν_s, stretching frequencies of the SiOSi bridge indicate the asymmetric force constant is greater. The asymmetric stretching frequency is expected to be higher since it involves a large amplitude of vibration for the lighter central atom and a small amplitude of vibration for the terminal groups. Conversely, ν_s should be low since the central atom has a small amplitude of vibration and the terminal groups have a large amplitude of vibration in the

---

[3]The $d(Si-O_{nb})$ =1.65 Å in this $H_6Si_2O_7$ cluster.

[4]The $d(Al-O_{nb})$ =1.735 Å in this $H_6Al_2O_7^{-2}$ cluster.

symmetric mode (Ross, 1972). Model I, however, predicts the opposite to what is expected.

In addition to comparing k_s and k_a, model I was used to study the effects that polymerization and substitution of Al for Si have upon the force constants at one bar and as a function of pressure. A comparison of asymmetric stretching force constants at atmospheric pressure for the dimers, $H_6Si_2O_7$ and $H_6Al_2O_7^{-2}$,and highly-polymerized clusters, $H_{12}Si_5O_4$ and $H_{12}AlSi_4O_4^{-1}$, is found in Table I. With increasing polymerization from $H_6Si_2O_7$ to $H_{12}Si_5O_4$, the asymmetric stretching force constant of $d(Si-O_b)$ does not increase significantly. Spectroscopic studies on framework silicates show asymmetric stretching frequencies for TOT linkages are in the range 950-1200 cm^{-1} (Milkey, 1960; Moenke, 1962; Lyon, 1962; Moenke, 1966). Furthermore, these values overlap the range found for pyrosilicates and chain silicates (Farmer, 1974) thus supporting our results.

A decrease in the asymmetric stretching force constant from 788 Nm^{-1} to 647 Nm^{-1} was found by substituting aluminum for silicon in the dimer. The cluster with AlOSi linkages, $H_{12}AlSi_4O_4^{-1}$, has an asymmetric stretching force constant of 695 Nm^{-1} which is less than that for the Si-O bond and greater than that for the Al-O bond showing that there is a gradual decrease in k_a as the aluminum content increases. In keeping with our results, Milkey (1960) has noted that the center of gravity of absorption bands in the region 950-1200 cm^{-1} tends to shift to lower frequency with increasing

Table I. Asymmetric stretching force constants (k_{ϖ}) calculated at 1 bar for the clusters $H_6Si_2O_7$, $H_6Al_2O_7^{-2}$, $H_{12}Si_5O_4$, and $H_{12}AlSi_4O_4^{-1}$ with all SiOSi and AlOSi angles equal to 180^0.

Cluster	k_{ϖ} (Nm^{-1})
$H_6Si_2O_7$	788
$H_6Al_2O_7^{-2}$	647
$H_{12}Si_5O_4$	796
$H_{12}AlSi_4O_4^{-1}$	695

aluminum content.

Calibration of pressure for the clusters studied with model I was not possible. We were, however, able to look at relative changes and values of the force constants with increasing pressure by plotting log(k) verses log(d(T...T) where d(T...T) is the intertetrahedral distance (Figure 3). As d(T...T) decreases the pressure increases, hence the pressure increases from right to left in Figure 3. The asymmetric stretching force constants for d(Al-O_b) are consistently lower than those for d(Si-O_b) with increasing pressure. In addition, the force constants for the dimers (Figure 3a) and the highly-polymerized clusters (Figure 3b) increase similarly with decreasing intertetrahedral distances as seen by the nearly parallel trends.

The use of model I verified the feasibility of studying Si-O bond energetics and force constants at simulated elevated pressures with _ab initio_ SCF molecular orbital calculations. The model was abandoned, however, in favor of model II which allows us to incorporate the important structural variable of the SiOSi angle.

Model II

With the SiOSi bending force constant and symmetric Si-O stretching force constant, we can solve equations (26), (27)

Figure 3. Log of the asymmetric Si-O stretching force constant, $\log(k_a)$, plotted against the inter-tetrahedral distance, $\log(\, d(T...T)\,)$, for $H_6Si_2O_7$ where $\log(k_a)=-7.35\log(Si...Si)+4.55$ ($r^2=0.999$); $H_6Al_2O_7^{-2}$ where $\log(k_a)=-7.42\log(Al...Al)+4.63$ ($r^2=0.998$); $H_{12}Si_5O_4$ where $\log(k_a)=-7.12\log(Si...Si)+4.47$ ($r^2=0.999$); and $H_{12}AlSi_4O_4^{-1}$ where $\log(k_a)=-7.41\log(Al...Si)+4.62$ ($r^2=0.998$).

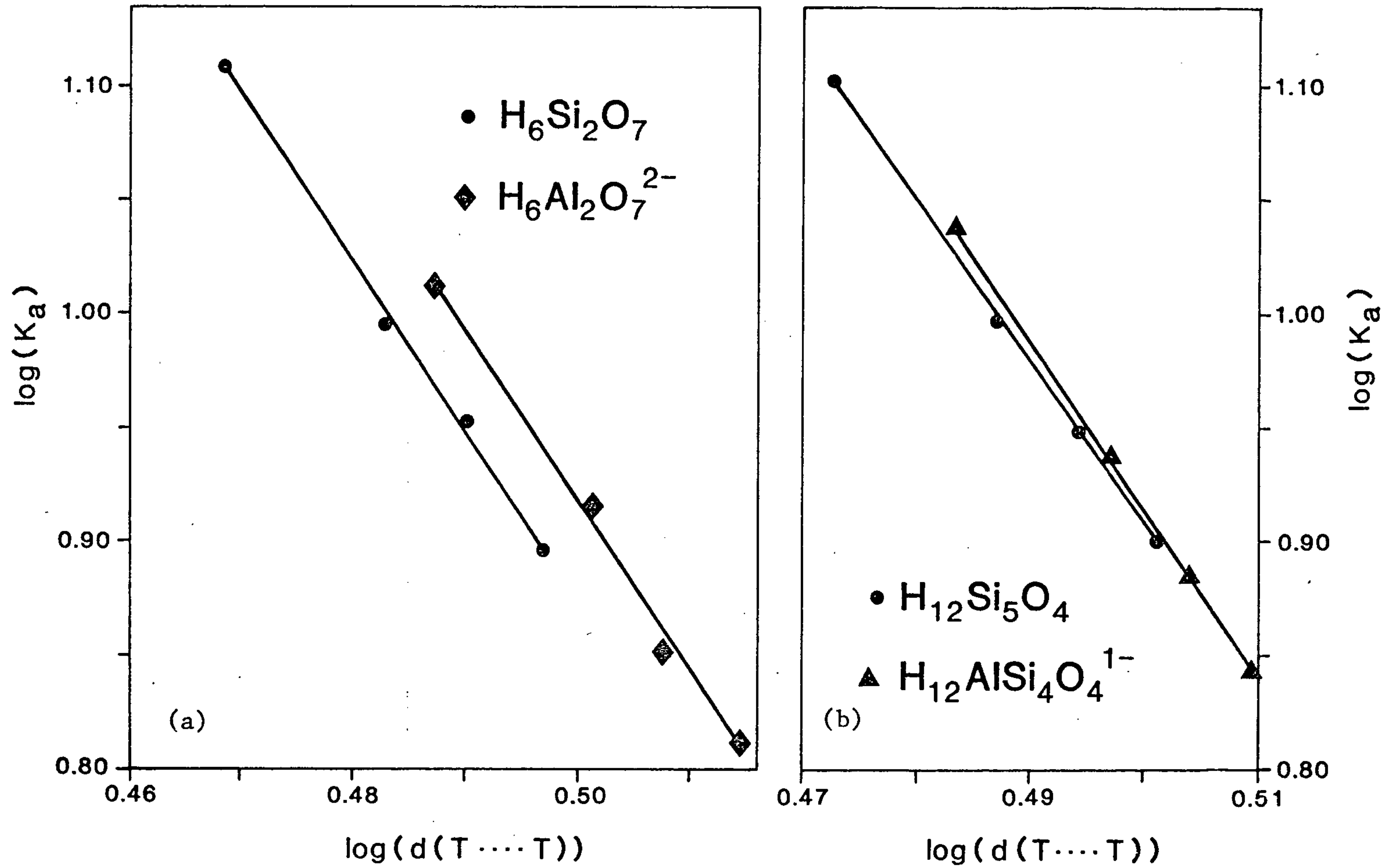

and (28) simultaneously for ν_a, ν_s and ν_b. Table II presents a comparison between the vibrational frequencies calculated for $H_6Si_2O_7$ at one bar and those determined from infrared and raman spectroscopic experiments at one bar for compounds containing SiOSi linkages. The $Si_2O_7^{-6}$ anion, siloxane, $(O(Si(CH_3)_2)_4$, and pyrosilicate, $Ba_2TiOSi_2O_7$, display a range of values for the principal vibrational frequencies. For example, ν_s varies from 503-665 cm^{-1} while ν_a ranges from 1029-1104 cm^{-1} . The only bending vibrational frequency attributed solely to SiOSi bending is 169 cm^{-1} for the $Si_2O_7^{-6}$ anion. The calculated values show a reasonable agreement with experimental data. The results are even more encouraging considering we are comparing the energetics of the SiOSi linkage in $H_6Si_2O_7$ with the energetics of the SiOSi linkage in very complex compounds. This lends further support to the premise that the local bonding forces in siloxanes and silicates are similar to those in isolated molecular clusters involving the same atoms and coordination number.

In Figure 4a, ν_a is plotted against the average bridging Si-O bond length for twelve pyrosilicates at atmospheric pressure (Farmer, 1974). A similar trend is found for $H_6Si_2O_7$ (Figure 4b) where the different d(Si-O_b) correspond to calculated equilibrium distances at different SiOSi angles. Both trends show a decrease in the asymmetric Si-O stretching frequency as d(Si-O_b) increases. Since ν_a is directly proportional to the square root of the symmetric stretching force constant (19), k_s also decreases as d(Si-O_b) increases.

Table II. Comparison at 1 bar of calculated symmetric stretch, ν_s, and asymmetric stretch, ν_a, and bending, ν_b, frequencies for $H_6Si_2O_7$ with those determined from infrared and raman spectra for $Si_2O_7^{-6}$, $(O(Si(CH_3)_2)_4$, and $BaTiOSi_2O_7$.

	Calculated Frequencies (cm^{-1})	Experimental Frequencies (cm^{-1})		
	$H_6Si_2O_7$	$Si_2O_7^{-6}$ [a]	$O(Si(CH_3)_2)_4$ [b]	$BaTiOSi_2O_7$ [c]
ν_s	588	503	547	665
ν_a	1252	1029	1104	1039
ν_b	133	169	---	---

[a] Gillespie and Robinson, 1964.

[b] Lazarev, 1972.

[c] Gabelica-Robert and Tarte, 1981.

Figure 4. A comparison of the asymmetric stretching frequency, ν_a, plotted against the bridging bond length, d(Si-O_b), for a group of twelve pyrosilicates (a) and $H_6Si_2O_7$ (b); ν_a's were determined from spectroscopic experiments for the pyrosilicates whereas ν_a's for $H_6Si_2O_7$ were calculated.

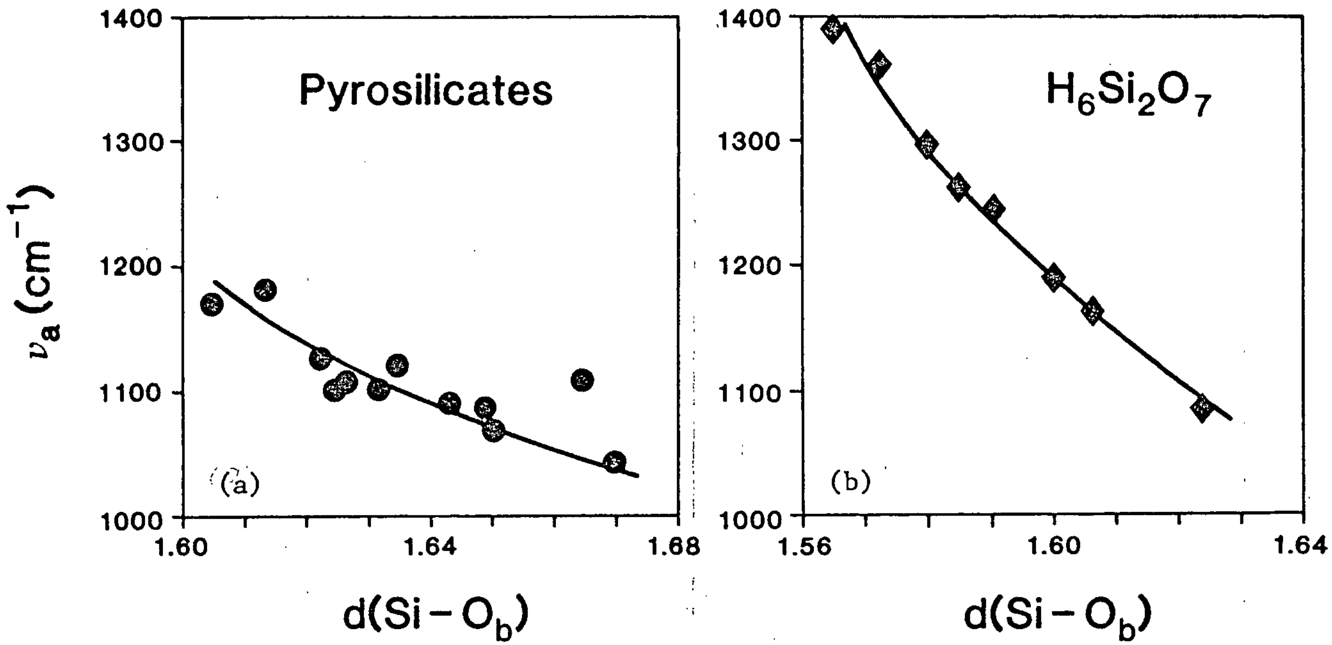

In other words, the bridging Si-O bond becomes more incompressible (that is, greater k_S) as the bridging bond length decreases.

The agreement between our calculations and experimental studies at atmospheric pressure was encouraging enough for us to proceed with the simulation of pressure. Because the equilibrium $d(Si\text{-}O_b)$ decreases as the bridging angle widens at one bar (Newton and Gibbs, 1980), constant $d(He\text{-}O_b)$ values do not represent equal pressures at different bridging angles. To approximate equivalent pressures for different angular configurations, Hooke's Law was employed and the fact that pressure is directly proportional to the force being applied. Therefore units of equivalent pressures equal to $k_{av}\Delta x$ were established where $k_{av}\Delta x$ is the average of the symmetric stretching force constant over the interval, Δx, studied. These provide reasonable approximations of equivalent pressures as long as the interval, Δx, is small.

Using this method, a potential energy surface for $He_2H_6Si_2O_7$ was constructed as a function of the bridging Si-O bond length and SiOSi angle at elevated pressure (Figure 5). This pressure is estimated to be 140 kbar by methods explained later. At one bar, the energy surface shows a long, narrow valley surrounded on three sides by steep energy barriers (Figure 5). The topology of the energy surface changes notably with pressure. At 140 kbar, the surface shows a distinct minimum surrounded on four sides by energy barriers which are significantly steeper than those at one bar.

Figure 5. Potential energy surfaces for $H_6Si_2O_7$ at 1 bar and 140 kbar plotted as a function of the bridging distance, d(Si-O_b), and the SiOSi angle.

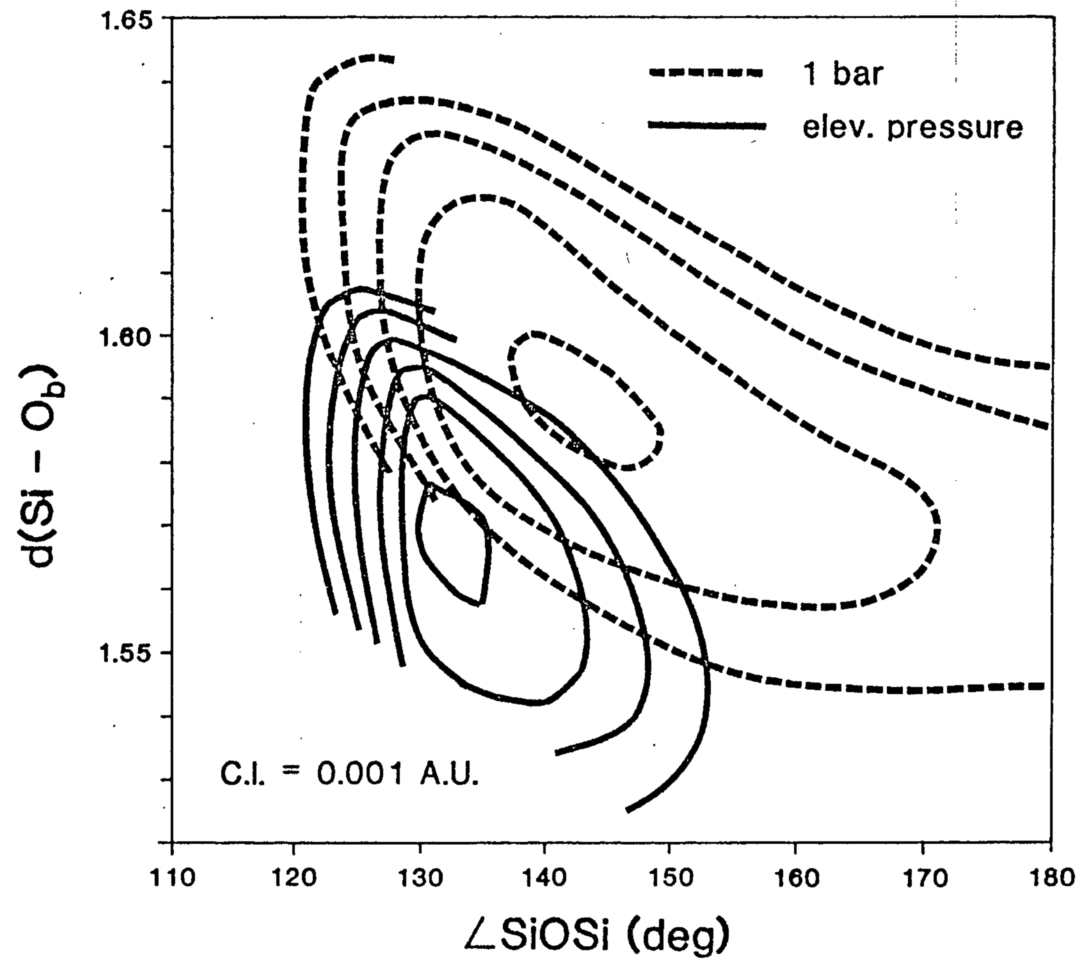

Comparing the minimum of the energy trough at one bar and 140 kbar, we see that there is a narrowing of the SiOSi angle from 142° to 132° and a decrease of the bridging Si-O bond from 1.585 Å to 1.565 Å. The steepening of the sides of the energy surface is reflected by the increase in k_s from 743 Nm^{-1} at one bar to 913 Nm^{-1} at 140 kbar (Figure 6) and an almost tripling of k_δ from 8.2 Nm^{-1} at one bar to 20.6 Nm^{-1} at 140 kbar (Figure 7). By taking vertical cross sections through the potential energy surfaces, the relationship between k_s and the SiOSi angle can be studied at one bar and 140 kbar. Figure 8 shows that k_s increases as the bridging angle widens at the two pressures. Earlier we investigated the relationship between and d(Si-O_b) at atmospheric pressure for $H_6Si_2O_7$ and a group of pyrosilicates (Figure 4) mentioning that ν_a is directly proportional to k_s. Newton and Gibbs (1980) have demonstrated at one bar that d(Si-O_b) is inversely correlated with the SiOSi angle. Therefore we are restating the relation between ν_a and d(Si-O_b) (Figure 4) in terms of k_s and the bridging angle (Figure 8); in addition, we predict that this relationship holds at pressure.

The increase in k_s and k_δ with pressure is supported by the infrared spectroscopic studies of Ferraro and Manghnani (1972) and Ferraro _et al_. (1972) on α-quartz and silicate glasses at pressures up to 58.8 kbar. They found that the intertetrahedral Si-O stretching frequency for α-quartz, fused silica, Vycor, and Pyrex shows a positive dependence with pressure. The mixed OSiO and SiOSi bending frequency for α-

Figure 6. A comparison of the potential energy curves for $H_6Si_2O_7$ plotted as a function of the bridging distance, d(Si-O_b), at 1 bar (upper curve) and 140 kbar (lower curve), where $He_2H_6Si_2O_7$ is the high pressure phase.

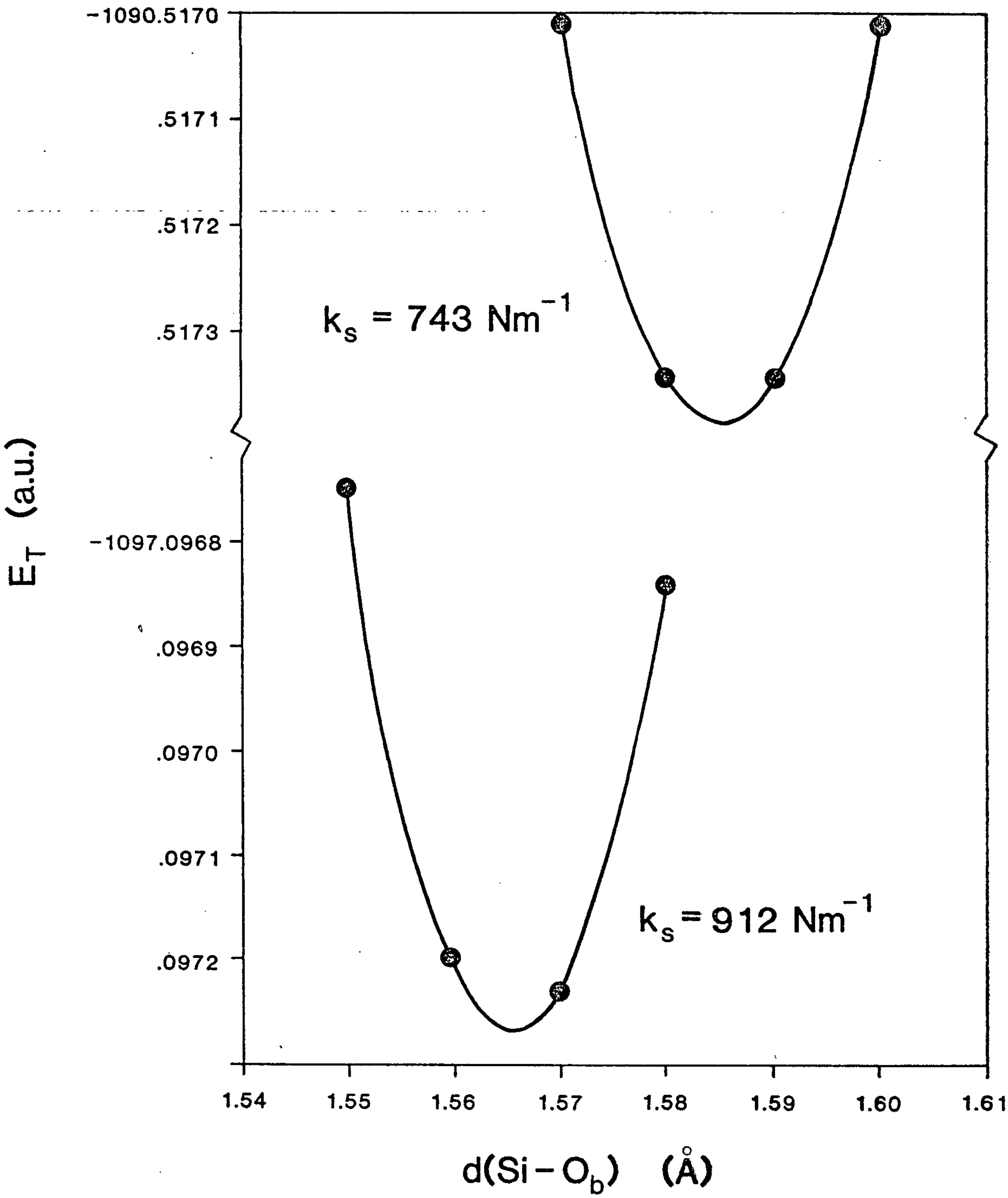

Figure 7. A comparison of the potential energy curves for $H_6Si_2O_7$ plotted as a function of the SiOSi angle at 1 bar (upper curve) and 140 kbar (lower curve), where $He_2H_6Si_2O_7$ is the high pressure phase.

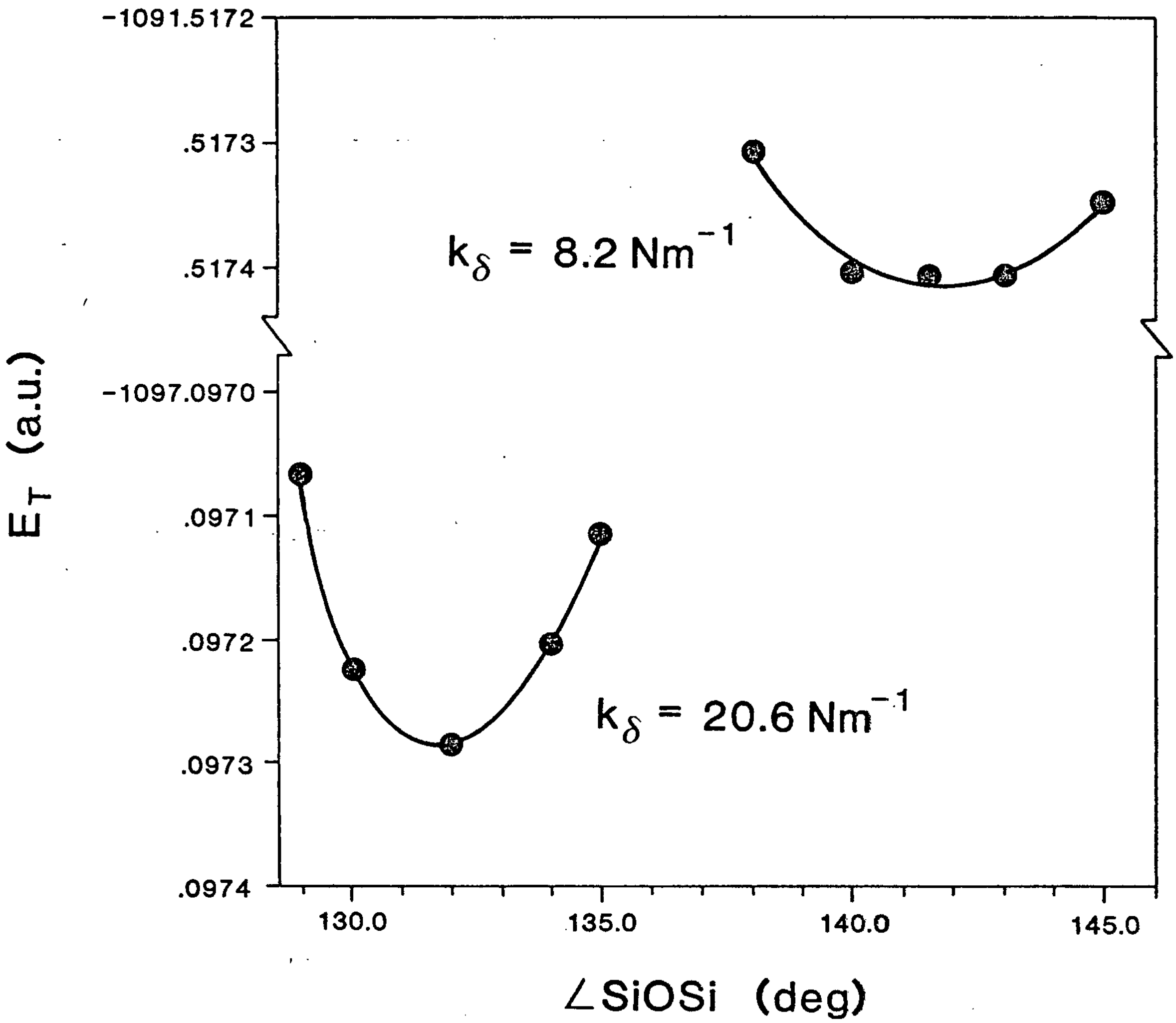

Figure 8. Symmetric Si-O stretching force constant, k_s, plotted against the SiOSi angle at 1 bar (left) where $k_s=0.038(\mathrm{SiOSi})+1.941$, $r^2=0.97$, and 140 kbar (right) where $k_s=0.040(\mathrm{SiOSi})+3.964$, $r^2=0.93$.

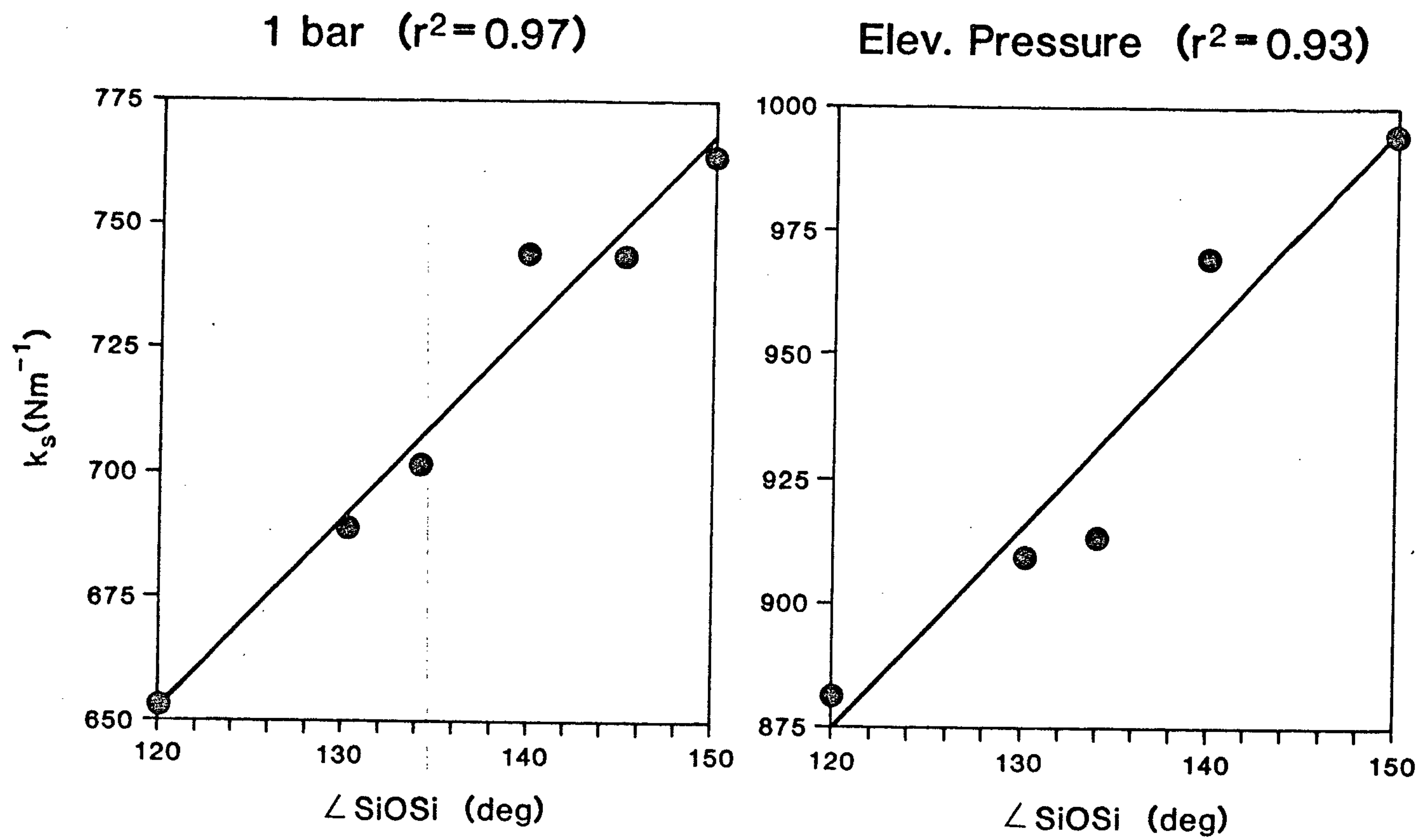

quartz also shows a positive dependence with pressure. The pressure dependence noted for this frequency primarily reflects the change of the SiOSi angle linking the tetrahedra. The results indicate that compression of glass takes place along network chains causing tetrahedra to move closer to one another (Ferraro _et al._ , 1972).

The change in SiOSi angle is the most prominent effect of pressure in our calculations, narrowing 7.0% for a pressure increment of 140 kbar while d(Si-O) decreases 1.3%. Recent high-pressure crystallographic studies of α-quartz (Jorgensen, 1978; Levien _et al._ , 1980) have also shown that the major effect of pressure on the structure is to close down the SiOSi angle. Between one bar and 61.4 kbar, Levien _et al._ (1980) found that the average Si-O bond length decreased 0.3% while the SiOSi angle decreased 6.6%. In this study, a comparative increase of 60 kbar resulted in a 0.3% decrease in $d(Si\text{-}O_b)$ and a 4.5% decrease in the bridging angle. Jorgensen (1978) and Levien _et al._ (1980) performed the high-pressure experiments under hydrostatic conditions. With an increase in pressure, the framework of corner-linked tetrahedra can be collapsed ideally (thereby reducing molar volume) by a cooperative tilting of the rigid tetrahedra in such a way that the tetrahedra remain undistorted; the SiOSi angle, however, is reduced significantly. In our calculations, a directed stress is imposed by helium atoms placed along the Si-O vectors. The reason for this intrinsic preference for a smaller SiOSi angle with increased pressure in the $He_2H_6Si_2O_7$

molecule is not apparent. The electronic adjustments with increasing pressure are minimal as can be seen in Table III. There is essentially no change in the Mulliken bond overlap population $n(Si-O_b)$ as well as the net charges on the bridging oxygen and silicons . Likewise gross charges on the valence orbitals of silicon and oxygen show no significant variation. The increasing negative values of n(Si...Si) (Table III) would tend to favor a wider SiOSi angle with increasing pressure. It is of interest, however, that the molecular group shows an intrinsic preference for smaller SiOSi angles unrelated to volume considerations.

Although $n(Si-O_b)$ exhibits no change with increasing pressure (Table III), it can be correlated with $d(Si-O_b)$ and k_S when pressure remains constant (Figure 9). An increase of the electronic overlap population between Si and O results in a shorter bond length and a concommittant increase in k_S at one bar and 140 kbar. Newton and Gibbs (1980) have demonstrated at one bar that $n(Si-O_b)$ shows a curvilinear trend when plotted against SiOSi but is linearly correlated with -sec(SiOSi). The latter correlation can be related to hybridization of the valence orbitals on the bridging oxygen of $H_6Si_2O_7$ (Brown et al. , 1969). If the hybrid orbitals on the oxygen are expressed in the form $s+\lambda p$ where λ is the s-p mixing coefficient, it can be shown that $\lambda^2=-\sec(SiOSi)$; furthermore, the SiOSi angle determines the percentage s-character, $100/(1+\lambda^2)$, of each hybrid (McWeeney, 1979). To investigate how pressure affects this relationship, $n(Si-O_b)$

Table III. Mulliken bond overlap populations, n(Si-O_b) and n(Si...Si), and atomic charges on bridging oxygen, Q(O_b), and silicon, Q(Si), for $H_6Si_2O_7$ at 1 bar , 60 kbar and 140 kbar; bridging Si-O bonds and SiOSi angle are optimized.

P (kbar)	n(Si-O_b)	n(Si...Si)	Q(O_b)	Q(Si)
1×10^{-3}	+0.50	-0.058	-0.70	1.57
60	+0.50	-0.060	-0.70	1.58
140	+0.50	-0.062	-0.71	1.59

Figure 9. Mulliken bond overlap population, $n(Si-O_b)$, plotted against the bridging distance, $d(Si-O_b)$, at 1 bar (a) and against the symmetric stretching force constant, k_s, at 1 bar (b) with r^2 values of 0.997 and 0.989, respectively; the corresponding relationships at 140 kbar are found in (c) and (d) with r^2 values of 0.999 and 0.971, respectively.

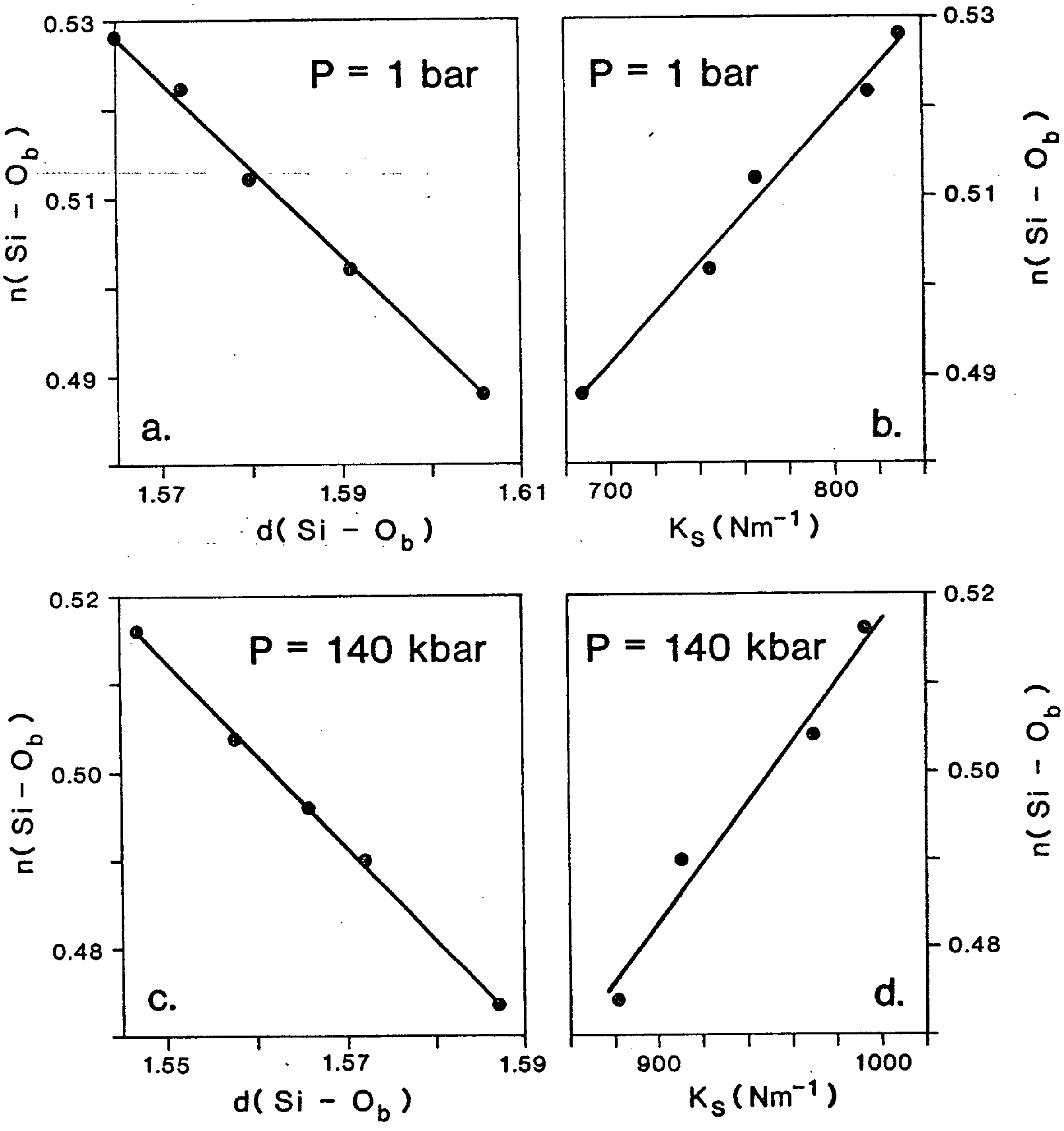

values were plotted against the bridging angle at one bar and 140 kbar (Figures 10a and 10c). The trends at both pressures are curvilinear. On the other hand, when $n(Si-O_b)$ was plotted against the percentage s-character of the bridging oxygen at the two pressures (Figures 10b and 10d), well-developed linear correlations ($r^2=0.996$ at 1 bar; $r^2=0.997$ at 140 kbar) were obtained.

A correlation closely related to the above is the relationship between $d(Si-O_b)$ and -sec(SiOSi). At atmospheric pressure, Newton and Gibbs (1980) have found that a linear correlation exists between $d(Si-O_b)$ and -sec(SiOSi). With increasing SiOSi, the s-character of the hybrid orbitals on the bridging oxygen increases and $d(Si-O_b)$ decreases. When observed Si-O bridging bond lengths in coesite are plotted against -sec(SiOSi) at one bar (Gibbs et al., 1977), a well-developed linear correlation ($r^2=0.96$) is obtained with the short bonds involving wide angles. It has been suggested (Levien et al., 1980; Levien and Prewitt, 1981) that this relationship fails to hold with increasing pressure. However, one would not expect the relation to hold for a given bond length with changing pressure; rather, one would expect the relation to hold for all bond lengths in a structure at constant pressure whether it be one bar or an elevated pressure. To investigate this, we undertook a study of the relationship between $d(Si-O_b)$ and -sec(SiOSi) at an elevated pressure. Figure 11 presents the results confirming our predictions that a significant linear correlation exists at a

Figure 10. Mulliken bond overlap population, $n(Si\text{-}O_b)$, plotted against the bridging SiOSi angle at 1 bar (a) and against the percentage s-character of the hybrid orbitals on the bridging oxygen, $100/(1+\lambda^2)$, at 1 bar (b) with the corresponding relationships at 140 kbar found in (c) and (d). The curvilinear trends in (a) and (c) both become linear in (b) and (d).

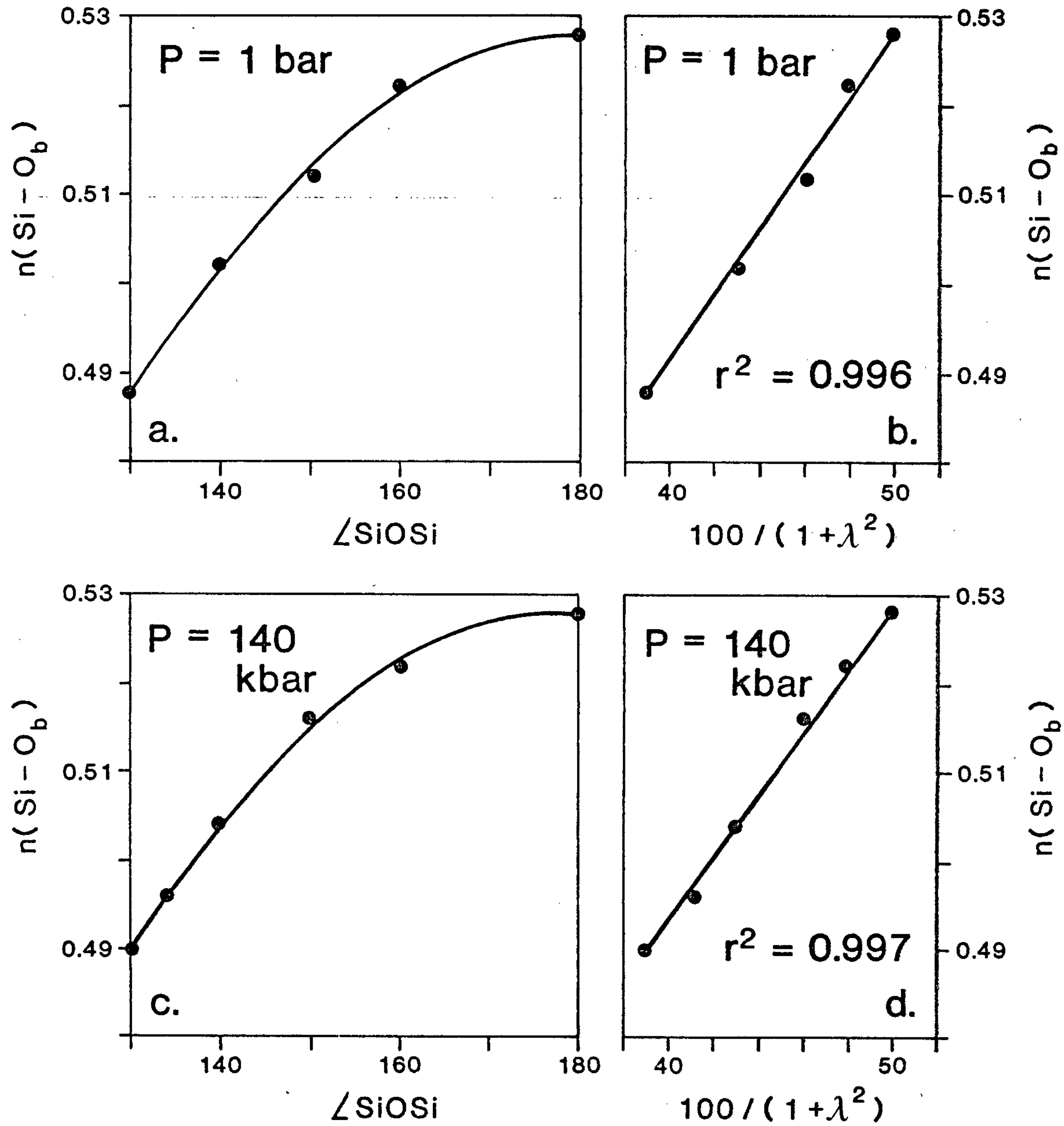

Figure 11. The relationship between the bridging Si-O distance and -sec(SiOSi) for $H_6Si_2O_7$ at 1 bar and an elevated pressure estimated to be 140 kbar.

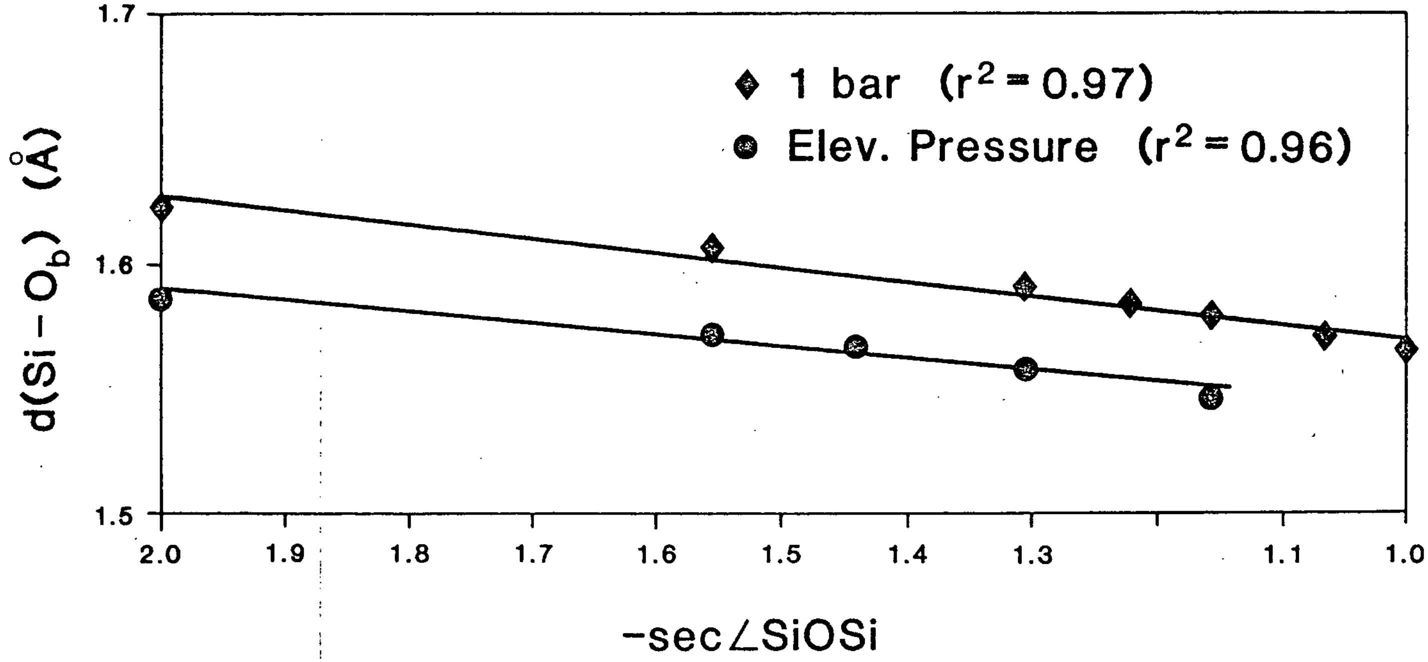

given high pressure (r^2=0.96) as well as 1 bar (r^2=0.97).

Recent work on the structure and compressibility of coesite at high pressure (Levien and Prewitt, 1981) supports this finding. When the average Si-O bridging bond lengths are plotted against -sec(SiOSi) at 51.9 kbar, a significant linear correlation (r^2=0.90) is found. Figure 12 compares the data for coesite at one bar and 51.9 kbar with the calculated data for $H_6Si_2O_7$ at one bar and 60 kbar. The agreement between experiment and theory is encouraging.

Estimates of pressure corresponding to $k_{av}\Delta x$ terms were obtained by modelling changes that occur in α-quartz with pressure. Levien et al. (1980) have noted a very slight decrease in the mean Si-O distance and a shift in the SiOSi angle from 143.7° to 134.2° for an increase of 61.4 kbar pressure. The $k_{av}\Delta x$ value corresponding to 61.4 kbar was approximated by keeping $d(Si\text{-}O_b)$ constant in $H_6Si_2O_7$ while decreasing SiOSi from 144° to 134°. Diagrammatically this is path A-C in Figure 13. Path B-C shows that there is a significant Δx associated with a change in pressure of 61.4 kbar. The value of 140 kbar for $k_{av}\Delta x$ used in many of the preceding calculations was estimated by extrapolation from the 61.4 kbar value.

Figure 12. A comparison between the average Si-O bridging distance plotted against -sec(SiOSi) for coesite (left) and $H_6Si_2O_7$ (right); at 1 bar and 52 kbar, the r^2 values for coesite based on experimental data from Levien and Prewitt (1981) are 0.97 and 0.90, respectively; the r^2 values based on calculations at 1 bar and 60 kbar for $H_6Si_2O_7$ are 0.97 and 0.98, respectively.

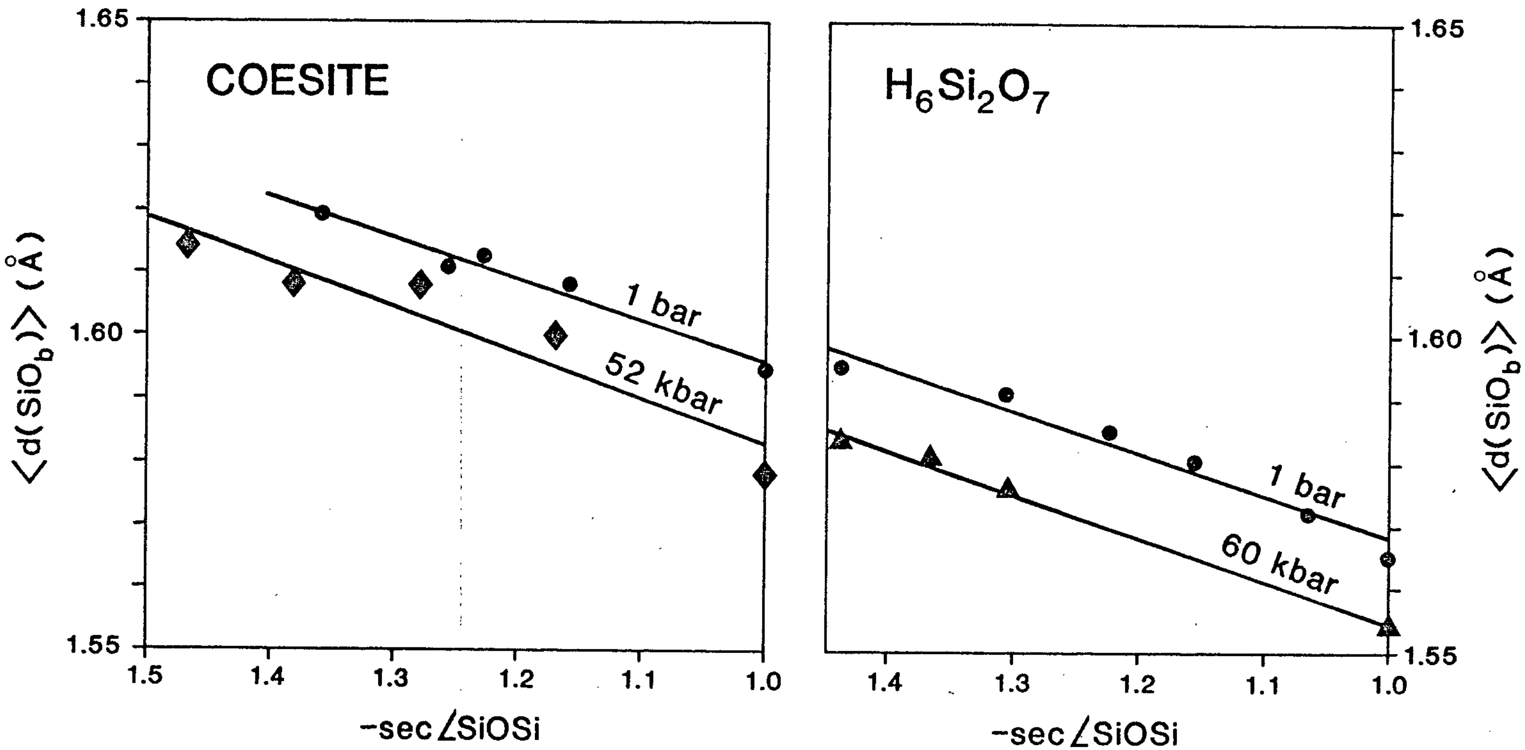

Figure 13. Illustration of how estimates of $k_{av}\Delta x$ roughly equivalent to 60 kbar pressure were obtained. Modelling changes that occur in -quartz at this pressure, d(Si-O_b) was kept constant while decreasing the SiOSi angle from 144° to 134° (path A-C); path B-C shows the x associated with an increment of 60 kbar pressure.

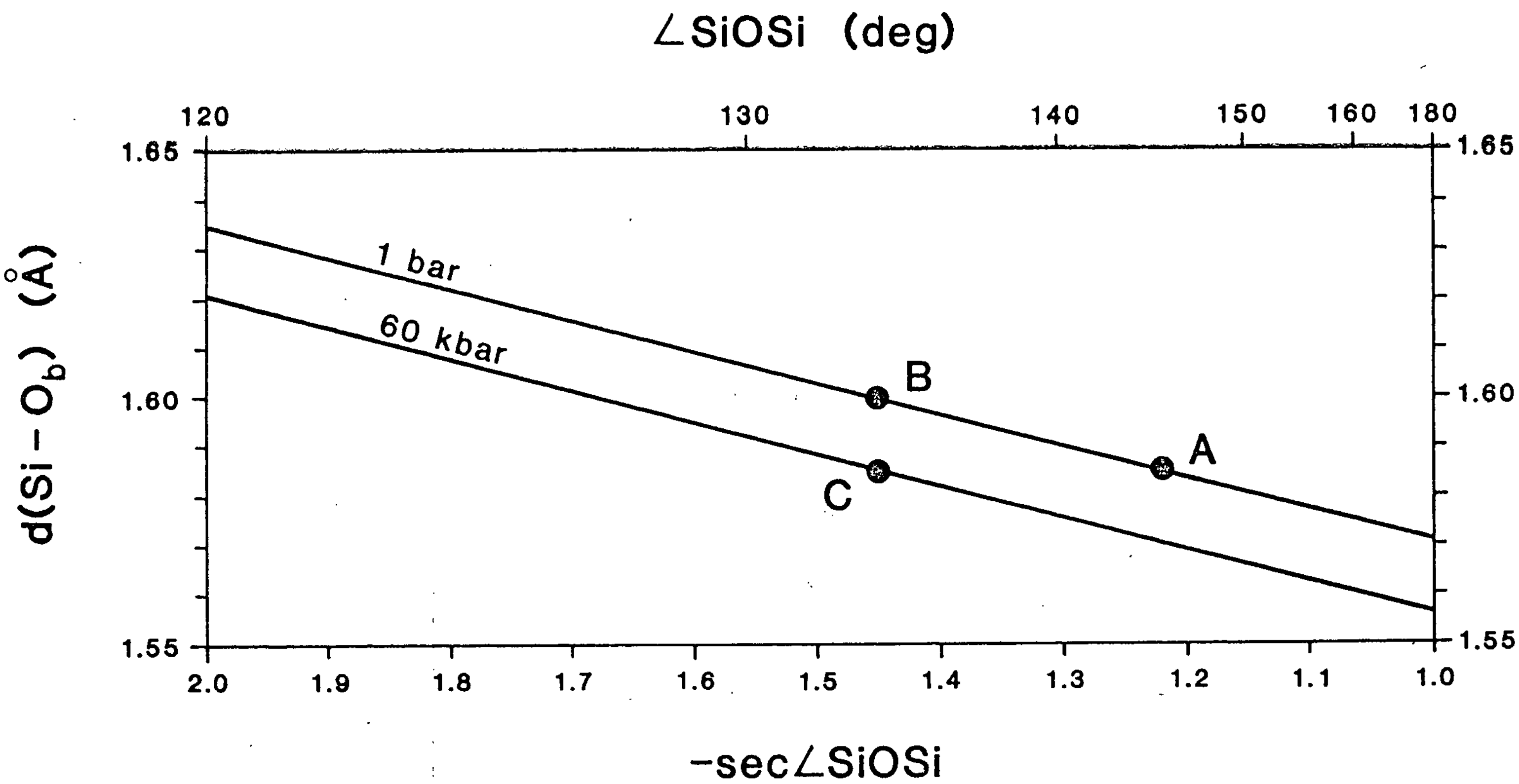

VI. CONCLUSIONS

Molecular orbital theory is a bonding formalism based upon quantum mechanical principles and has been applied to mineralogical studies of equilibrium molecular geometry, electronic charge distributions, electronic spectra and force constant calculations. To date, these studies have been limited to one atmosphere pressure. With the ever increasing interest in ultra-high pressure phases and mantle mineralogy, bonding studies of molecular groups at simulated high pressure can be an invaluable aid to understanding high pressure crystal chemistry, bond energetics and electronic spectra. In addition, such studies will enable us to simulate pressures beyond the limits of current experimental technology.

This investigation is devoted to the study of equilibrium Si-O bond lengths, SiOSi angles and Si-O force constants with increasing pressure. Although the method of applying pressure is rather crude in that helium atoms are used to apply a directed stress axial with the Si-O bridging bond length, we feel the results are reasonable approximations of expected trends. For example, with increasing pressure the Si-O bond length and SiOSi angle decrease 0.3% and 4.5% , respectively, up to 60 kbar pressure which compares well with the 0.3% and 6.6% decrease observed in α-quartz (Levien _et_ _al_. , 1980). Furthermore, the linear correlation of Si-O bond length and -sec(SiOSi), known to occur at one atmosphere, holds at increased pressure; this trend is also observed in coesite at high pressures.

Symmetric Si-O stretching and SiOSi bending force constants show a percentage increase in the ratio of 1:6 up to an estimated pressure of 140 kbars which is in keeping with the relative decrease in d(Si-O_b) and the SiOSi angle. Experimentally determined stretching and bending force constants in silicates at high pressure are sparse. Ferraro et al. (1972) and Ferraro and Manghnani (1972) have investigated the infrared spectra of α-quartz, fused silica, Pyrex, Vycor and a variety of sodium silicate glasses at pressures up to 58.8 kbar. The absorption bands attributed to Si-O-Si stretch vibrations show, in general, a positive dependence with pressure indicating a corresponding increase in the stretching force constant. Similarly the mixed bending frequency of the SiOSi and OSiO angles shows a positive dependence with pressure for α-quartz and the sodium silicate glasses; the positive pressure dependence noted for this frequency primarily reflects the change in the SiOSi angle (Ferraro et al., 1972) and indicates that the SiOSi bending force constant is increasing with pressure.

Although this study has focused on the $H_6Si_2O_7$ cluster, it represents the initial installment in a series of studies on the compressibilities of geologically important metal-oxygen polyhedra. Work is currently in progress on the H_4SiO_4 and $H_4AlO_4^{-1}$ tetrahedra and we are calculating force constants, polyhedral bulk moduli, Kp, as well as the first derivative of Kp with respect to pressure, d(Kp)/dP. Future work will be devoted to force constant, Kp and d(Kp)/dP determinations for oxyanion clusters of magnesium, aluminum and silicon in octahedral coordination. Ultimately we hope to approximate the bulk modulus of a solid phase at high pressure through computed Kp and bending force constants.

REFERENCES

Binkley, J.S., R. Whiteside, P.C. Haribaran, R. Seeger, W.J. Hehre, W.A. Lathan, M.D. Newton, R. Ditchfield, and J.A. Pople, 1978, Gaussian 76- an ab initio molecular orbital program: Quantum Program Chemical Exchange, Bloomington, IN.

Brown, G.E., G.V. Gibbs and P.H. Ribbe, 1969, The nature and variation in length of the Si-O bond and Al-O bonds in framework silicates: Am. Mineral., 54, 1044-1061.

Cameron, M., S. Sueno, C.T. Prewitt and J.J. Papike, 1973, High temperature crystal chemistry of acmite, diopside, hedenbergite,jadeite, spodumene and ureyite: Am. Mineral., 58, 594-618.

Collins, J.B., P. Von R. Schleyer, J.S. Binkley and J.A. Pople, 1976, Self-consistent molecular orbital methods. XVII. Geometries and binding energies of second row molecules. A comparison of three basis sets: Jour. Chem. Phys., 64, 5142-5151.

De Jong, B.H.W.S. and G.E. Brown, 1980, The polymerization of silicate and aluminate tetrahedra in glasses, melts and aqueous solutions-I. Electronic structure of $H_6Si_2O_7$, $H_6AlSiO_7^{1-}$ and $H_6Al_2O_7^{2-}$: Geochim. Cosmochim. Acta, 44, 491-511.

Farmer, V.C., ed., 1974, The infra-red spectra of minerals: Mineral. Soc. London, 539 p.

Ferraro, J.R. and M.H. Manghnani, 1972, Infrared absorption spectra of sodium silicate glasses at high pressures: Jour. Appl. Phys., 43, 4595-4598.

Ferraro, F.R., M.H. Manghnani and A. Quattrochi, 1972, Infrared spectra of several glasses at high pressures: Phys. Chem. Glasses, 13, 116-121.

Gibbs, G.V., E.P. Meagher, M.D. Newton and D.K. Swanson, in press, A comparison of experimental and theoretical bond length and angle variations for minerals, inorganic solids and molecules: 34 p. In O'Keeffe, M. and A. Navrotsky (eds.), Structure and bonding in crystals: Academic Press, New York.

Gibbs, G.V., C.T. Prewitt and K.J. Baldwin, 1977, A study of of structural chemistry of coesite: Zeit. Kristall., 145, 108-123.

Gillespie, R.J. and E.A. Robinson, 1964, Characteristic frequencies of compounds containing Si-O-Si, P-O-P, S-O-S and vibrational Cl-O-Cl bridging groups: Can. Jour. Chem., 42 , 2496-2503.

Hazen, R.M. and L.W. Finger, 1979, Bulk modulus-volume relationship for cation-anion polyhedra: Jour. Geophys. Res., 84 , 6723-6728.

Hehre, W.J., R.F. Stewart and J.A. Pople, 1969, Self-consistent molecular orbital methods. I. Use of Gaussian expansions of Slater-type atomic orbitals: Jour. Chem. Phys., 51 , 2657-2664.

Herzberg, G., 1945, Infrared and raman spectra of polyatomic molecules, vol. 2: D. Van Nostrand Co., New York, 632 p.

Jezowska-Trzebiatowska, B., J. Hanuza and W. Wojciechowski, 1967, Infra-red and vibrational frequencies of the X-O-X bonds for the IVth periodic group of elements: Spectrochim. Acta, 23A , 2631-2636.

Jorgensen, J.D., 1978, Compression mechanisms in α-quartz structures- SiO_2 and GeO_2: Jour. Appl. Phys., 49 , 5473-5478.

Lazarev, A.N., 1972, Vibrational spectra and structures of silicates, translated from Russian: Consultants Bureau, New York, 302 p.

Levien, L. and C.T. Prewitt, 1981, High-pressure crystal structure and compressibility of coesite: Am. Mineral., 66 , 324-333.

Levien, L., C.T. Prewitt and D.J. Weidener, 1980, Structure and elastic properties of quartz at pressure: Am. Mineral., 65 , 920-930.

Louisnathan, S.J. and G.V. Gibbs, 1972, Variation of Si-O distances in olivines, sodamelilite and sodium metasilicate as predicted by semi-empirical molecular orbital calculations: Am. Mineral., 57 , 1643-1663.

Lyon, R.J.P., 1962, Minerals in the infrared: Stanford Research Institute, California.

McWeeney, R., 1979, Coulson's valence: Oxford Univ. Press, Oxford, 434 p.

Meagher, E.P., J.A. Tossell and G.V. Gibbs, 1979, A CNDO/2 molecular orbital study of the silica polymorphs quartz, cristobalite and coesite: Phys. Chem. Min., 4 , 11-21.

Milkey, R.G., 1960, Infrared spectra of some tectosilicates:

Am. Mineral., 45 , 990-1003.

Moenke, H., 1962, Mineralspektren,I.: Akademie-Verlag, Berlin.

Moenke, H., 1966, Mineralspektren,II.: Akademie-Verlag, Berlin.

Mulliken, R.S., 1955, Electronic population analysis on LCAO-MO molecular wave functions. I.: Jour. Chem. Phys., 23 , 1833-1840.

Newton, M.D. and G.V. Gibbs, 1980, Ab initio calculated geometries and charge distributions for H_4SiO_4 and $H_6Si_2O_7$ compared with experimental values for silicates and siloxanes: Phys. Chem. Min., 6 , 221-246.

Newton, M.D., W.A. Lathan, W.J. Hehre and J.A. Pople, 1970, Self-consistent molecular orbital methods. V. Ab initio calculation of equilibrium geometries and quadratic force constants: Jour. Chem. Phys., 52 , 4064-4072.

Newton, M.D., M. O'Keeffe and G.V. Gibbs, 1980, Ab initio calculation of interatomic force constants in $H_6Si_2O_7$ and the bulk modulus of α-quartz and α-cristobalite: Phys. Chem. Min., 6 , 305-312.

Ohashi, Y. and C.W. Burnham, 1972, Electrostatic and repulsive energies of the M1 and M2 cation sites in pyroxenes. Jour. Geophys. Res., 77 , 5761-5766.

Papike, J.J., ed., 1969, Pyroxenes and amphiboles. Crystal chemistry and phase determinations: Mineral. Soc. Am. Special Paper, 2.

Pauling, L., 1980, The nature of the silicon-oxygen bonds: Am. Mineral., 65 , 321-323.

Pople, J.A., D.P. Santry and G.A. Segal, 1965, Approximate self- consistent molecular orbital theory. I. Invariant procedures: Jour. Chem. Phys., 43 , S129-S135.

Ross, S.D., 1972, Inorganic infrared and raman spectra: McGraw- Hill Book Co. (UK) Lmtd., London, 448 p.

Tossell, J.A., 1973, Molecular orbital interpretation of x-ray emmission and ESCA spectral shifts in silicates: Jour. Phys. Chem. Solids, 34 , 307-319.

Tossell, J.A., 1979, Diverse chemical bond types in minerals: Trans. Am. Crystall. Assoc., 15 , 47-63.

Tossell, J.A. and G.V. Gibbs, 1977, Molecular orbital studies of geometries and spectra of minerals and inorganic compounds: Phys. Chem. Min., 2 , 21-57.

Whittaker, E.J.W., 1971, Madelung energies and site preferences in amphiboles,1: Am. Mineral., 56 , 980-996.